

Boosting Large-scale Parallel Training Efficiency with C4 : A Communication-Driven Approach

Jianbo Dong, Bin Luo, Jun Zhang, Pengcheng Zhang, Fei Feng, Yikai Zhu, Ang Liu, Zian Chen, Yi Shi, Hairong Jiao, Gang Lu, Yu Guan, Ennan Zhai, Wencong Xiao, Hanyu Zhao, Man Yuan, Siran Yang, Xiang Li, Jiamang Wang, Rui Men, Jianwei Zhang, Huang Zhong, Dennis Cai, Yuan Xie, Binzhang Fu
Alibaba Group
jianbo.djb@alibaba-inc.com

Abstract

The emergence of Large Language Models (LLMs) has necessitated the adoption of parallel training techniques, involving the deployment of thousands of GPUs to train a single model. Unfortunately, we have found that the efficiency of current parallel training is often suboptimal, largely due to the following two main issues. Firstly, hardware failures are inevitable, leading to interruptions in the training tasks. The inability to quickly identify the faulty components results in a substantial waste of GPU resources. Secondly, since GPUs must wait for parameter synchronization to complete before proceeding to the next round of computation, network congestions can greatly increase the waiting time for GPUs. To address these challenges, this paper introduces a communication-driven solution, namely the C4 . The key insights of C4 are two folds. First, in parallel training, collective communication exhibits periodic and homogeneous characteristics, so any anomalies are certainly due to some form of hardware malfunction. By leveraging this feature, C4 can rapidly identify the faulty components, swiftly isolate the anomaly, and restart the task, thereby avoiding resource wastage caused by delays in anomaly detection. Second, the predictable communication model of collective communication, involving few large flows, allows C4 to efficiently execute traffic planning, substantially reducing network congestion. C4 has been extensively implemented across our production systems, cutting error-induced overhead by roughly 30% and enhancing runtime performance by about 15% for certain applications with moderate communication costs.

1 Introduction

The rapid advancement of Large Language Models (LLMs) [2, 5, 14, 41, 42, 49] has significantly impacted the fields of machine learning and artificial intelligence. LLMs such as GPT-3 [41] and Llama [49] are exhibiting human-like proficiency in text generation, question-answering, and even code creation. Despite the promising capabilities of these models, training them to reach their full potential is a complicated and resource-intensive process. Training a GPT-like model that has 175 billion parameters, for example, may require up to two months in a cluster of 1000 GPUs.

A key challenge in training LLMs in production AI clusters is that the effective utilization of GPU is relatively low, due to the following two reasons. First, a substantial amount of time is consumed in diagnosing system errors throughout the training lifespan due to the high failure rate of cutting-edge GPU products [32, 34]. Prolonged training sessions necessitate a stable process; however, the latest generation GPUs tend to exhibit high error rates, likely a consequence of their rapid development, rushed delivery, and increased power consumption. When running in Bulk Synchronous Parallel (BSP) [50] mode, errors in any node can cause the entire job to fail. This necessitates extensive time for system diagnosis and node isolation before we restart the job.

Furthermore, tuning the training process of these models to peak efficiency is a complex task, with communication costs being a significant impediment to scalability. That is, GPUs may experience delays at synchronization points while awaiting the outcomes of collective operations. The state of the arts suggest managing network traffic to improve communication performance. However, a shared physical cluster with multiple tenants running concurrent training jobs adds to the complexity of these patterns, exacerbating the difficulty in effective management. Additionally, the appearance of downlinks, which is increasingly common in large-scales systems, also diminishes the efficacy of previous traffic engineering strategies.

This paper proposes C4 (Calibrating Collective Communication over Converged Ethernet), an innovative system designed to unleash the computational capabilities of massive collaborating GPUs in large-scale AI clusters. C4 is composed of two subsystems, including C4D (C4 Diagnosis) and C4P (C4 Performance). C4D aims to enhance training stability by reducing stalls caused by uncorrectable errors. C4D achieves this by automatically detecting system errors in real-time, isolating faulty nodes, and facilitating application restarts from the last checkpoint. C4D’s innovation includes the following designs. (1) We enhance the collective communication library to offer the capability to monitor its status when running collective operations. (2) By collecting and analyzing the monitored status from different workers, we could detect the potential errors when one or some of ranks present suspected syndromes. (3) Once a suspect rank/node is reported, we could automatically isolate it from the scheduling system,

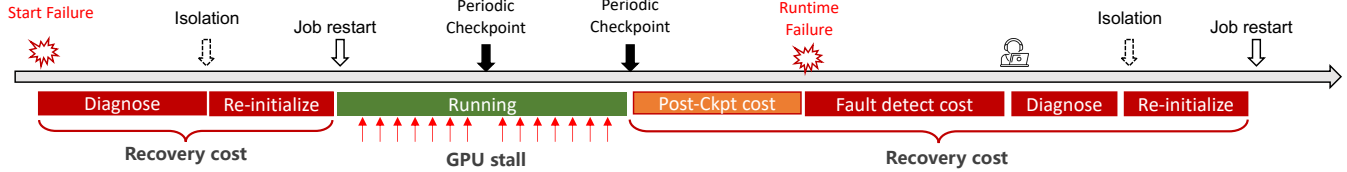


Figure 1. Problems that may occur in the lifetime of AI training applications.

and restart the job from last checkpoint. (4) C4D also collects the data from other system monitors, including the job monitor, server monitor, and network monitor, and conduct offline analysis accordingly.

C4P is designed to reduce the collective communication cost within large-scale training clusters. It accomplishes this by uniformly distributing network connections across all available paths and dynamically adjusting the load on each path based on the real-time network conditions. The key challenges it addresses include managing concurrent jobs and handling link errors. The novelty of C4P lies in the following aspects: (1) The communication library is enhanced with the ability to request path allocation prior to establishing connections. This feature enables it to control the designated communication paths for each link and to dynamically redistribute the network load across these paths. (2) C4P incorporates a mechanism for monitoring the integrity of network links, allowing it to identify and exclude faulty links from being considered in future path allocations, thereby maintaining network health and reliability. (3) For every communication request, C4P selects an optimal path, taking into account the current load distribution across all available network paths, ensuring efficient and balanced utilization of network resources.

C4 has been deployed in our AI training clusters for six months, and is now serving over 20 customers for LLM training. Leveraging its automatic error detection and recovery system, C4 effectively removes the majority of error-induced overhead, typically accounting for about 30% of the total time. Additionally, C4 mitigates the communication costs associated with imbalanced traffic. For the tested applications with modest communication cost, the throughput of jobs can be improved by approximately 15%. Collectively, these improvements result in an overall boost in cluster compute efficiency from 30% to 45%.

2 Challenges and Opportunities

Our team has successfully deployed numerous AI clusters, equipped with hundreds of thousands of GPUs, to enable a wide range of concurrent AI training jobs. In contrast to conventional cloud services, we have observed a pronounced difference in the expected delivery standards. That is, the users of AI clusters demand that their tasks perform at peak efficiency due to the following two reasons. First, the value of the developed models is intrinsically tied to how swiftly

they can be brought to market, making expedited training a priority. Second, the significant capital invested in the training infrastructure means that any performance degradation translates directly into substantial financial repercussions. However, maintaining a consistently perfect operating state for these large-scale systems proves challenging over extended periods, especially when the number of GPUs in a single job grow to thousands, or even tens of thousands.

The key challenges that forbid distributed training system operate in their peak performance include two aspects, as shown in Fig. 1. Firstly, the GPU worker may not be in the running state because of the occurrence of errors. Moreover, the GPU workers could wait for the completion of gradients synchronization and waste their computing power, even in running state.

Challenges and Opportunities in Error Handling. The distributed training jobs are sensitive to errors, because of the synchrony of collective communication. That is, any corrupted worker could cause the jobs to fail. To keep the training job moving forward, the users save checkpoints in run-time. And it will fallback to last valid checkpoint, if the job fails by some reasons. As shown in Fig. 1, critical errors can arise before or during the execution of DL training jobs. And they will affect the system utilization in different ways. If the defects exists before the start of training jobs, they will incur extra time spending on system diagnosing, error component isolation, and job restart. In this case, a lot of time is spent on system diagnosing and pinpointing the defect components, which may take hours or even days. While if the uncorrectable errors are encountered during the execution of training jobs, some more extra time is wasted, including the post-checkpoint cost and fault detection cost. Since the job must revert to the last valid checkpoint following an uncorrectable fault, the execution time after the last checkpoint is rendered futile. We refer to this as the post-checkpoint cost. Additionally, there is a delay between the occurrence of an error and its detection by users, which we term the fault detection cost.

Tab. 1 shows the statistics summary of errors encountered over a month by a representative job six months ago. The data indicates that the job experienced 40 crashes within that month due to these errors. In lack of efficient fault detection and diagnosing tools at that time, it can take hours to days to identify the root causes and pinpoint the defect nodes. Based on our experience, approximately 30% of time was

Table 1. Errors classification in AI training clusters.

Users' View	Root Causes	Error Rate	Localized
NCCL Error	Cuda Error	12.5%	100%
NCCL Error	ECC/NVLink Error	27.5%	100%
NCCL Error	NCCL timeout	20%	75%
NCCL Error	ACK timeout	27.5%	81.8%
Network Error	Others	12.5%	40%

expanded on error detection, system diagnosis, isolating defective nodes, and restarting processes, which left only 70% of the time available for actual computing tasks.

Users typically perceive most error types as a generic “NCCL Error”, making it challenging to pinpoint the exact root causes and respond to the reported errors effectively. For example, hardware issues in a GPU might cause one of the worker processes to crash. As a result, its peer workers fail to receive an acknowledgment after sending a message to the crashed worker, leading to an error code of 12 being thrown by the communication library. This same error code could also arise from other issues such as network disconnections, memory overflows causing container eviction, or even user code errors, such as tensor size mismatches. A key insight from the table is that the majority of errors (about 82.5%), are confined to specific nodes or even individual devices, suggesting the possibility of isolating the localized faulty components. This isolation strategy could prevent subsequent jobs from being impacted by the same faults.

To minimize recovery costs, it is essential to address each contributing factor appropriately. For swift diagnosis, our system automatically identifies defective nodes by leveraging the inherent characteristics of deep learning training jobs, such as balanced computing costs within a data parallel group and synchronization between iterations. Upon locating a defect, the system promptly initiates isolation and restart procedures, deferring in-depth root cause analysis to offline processing. To decrease the time spent on fault detection, human intervention should be eliminated, expediting the process from tens of minutes to mere seconds. In addition, to curtail the post-checkpoint cost, we have implemented a rapid checkpointing mechanism, similar to the prior work [51], capable of saving checkpoints approximately every 10 iterations.

Challenges and Opportunities in Optimizing Communication Performance. In addition to uncorrectable faults leading to job crashes, GPUs can experience stalls due to delays in completing collective operations or data loading tasks. This paper concentrates on addressing unnecessary overhead in collective operations. To begin with, elevated communication costs may arise from traffic collision among various flows or hardware issues, such as degraded PCIe lanes or Ethernet link failures. To simultaneously expand the maximum system scale and improve system availability and maintainability, we have adopted dual-port Network

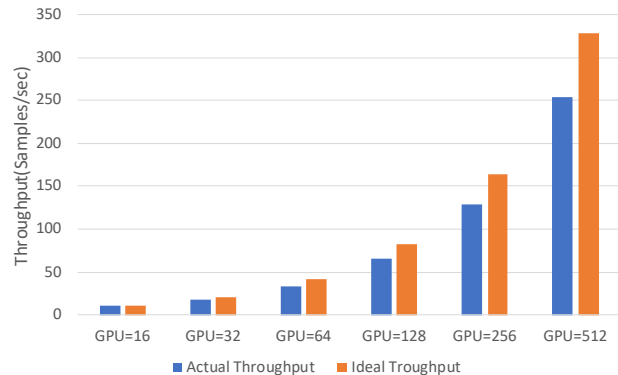


Figure 2. Scalability loss grows with the scale of systems.

Interface Cards (NICs) for system interconnects, with two separate ports bonded together. Having each port connecting to a distinct leaf switch, there would be two available links between the hosts and leaf switches. Should one link become inoperative, the remaining link would take over all the downstream traffic, making it a bottleneck in the system. Furthermore, beyond the communication overhead caused by hardware defects, there is also the potential for multiple data flows to compete for the available bandwidth of a single link. For today’s distributed training jobs, bandwidth constraints can significantly prolong the communication latency and lead to degradation of communication performance. As modern models and the training clusters grow in scale, this problem would be further exacerbated. Fig. 2 presents a comparison of actual versus ideal performance, training a representative GPT-like model composed of 22 billion parameters. It is evident that there exists a discrepancy between the effective performance achieved and the theoretical ideal performance, and this disparity amplifies as the scale of the system increases. Notably, when the system scales to 512 GPUs, the effective performance drops to 30% below the ideal performance.

Our analysis reveals that communication patterns in DL training clusters markedly differ from those in traditional cloud environments. In conventional cloud settings, we commonly observe a large number of concurrent connections, often several tens of thousands per instance. Such a volume of connections can be distributed across the network with relatively low variation using the Equal-Cost Multi-Path (ECMP) [19] routing strategy. Conversely, in distributed training systems, there are only a few longer-lasting connections, with each node typically managing around a few hundred connections. Traffic collisions in this environment can lead to substantial variations in the effective bandwidth of these connections, resulting in multi-fold increases in communication delays. However, this challenge is accompanied by an opportunity: the limited number of connections and their predictable patterns in DL training clusters offer a

unique advantage for enhancing communication efficiency through comprehensive global traffic engineering.

In essence, the effective performance of large-scale training clusters is significantly influenced by hardware defects and traffic collisions. To ensure that GPUs operate efficiently during model computation, it is critical to minimize the time lost in fault detection and system diagnosis. Furthermore, to prevent GPU stalls during periodic synchronization, it is essential to eliminate any superfluous communication overhead.

3 Design

In this section, we will elaborate on how our AI infrastructure tackles the two fundamental challenges identified earlier: ensuring stability and optimizing the performance of parallel training. We will explain the rationale behind our choice of system architecture, the compromises we have accepted, and offer an in-depth analysis of the particular technical hurdles we encountered.

3.1 Stability of Parallel Training

As indicated in Section 2, the GPU cluster’s resource utilization faces challenges due to increasing task sizes and hardware instability. With task scaling being an ongoing trend, we must address hardware failures through two strategies: 1) decreasing hardware failure rates and 2) systematically tolerating such failures. The first strategy is crucial but beyond this paper’s scope, and we briefly mention that temperature control is key (*Takeaways-1*). Methods like Dynamic Voltage and Frequency Scaling (DVFS) help prevent GPU overheating but can affect performance consistency. We improved cooling with faster fans and better air conditioning, achieving temperature regulation with minimal cost impact. The industry is moving towards more efficient cooling solutions like liquid cooling in future AI infrastructures.

Regarding the second strategy, we have attempted numerous solutions in collaboration with related teams. In general, traditional cloud applications employ online fault tolerance solutions. For instance, they tolerate computational faults by using redundant computations [30, 39, 48], provide highly reliable storage through erasure coding (EC) [1, 11, 53, 54] and/or triple-replica techniques, and endure network anomalies through multi-path (dual uplinks) strategies [18, 27]. However, for high-performance computing applications, the current mainstream approach is to use offline fault tolerance methods [23]. For example, applications periodically save checkpoints, and when a system failure occurs, the tasks are restarted from the last checkpoint. Of course, all computations between the last checkpoint and the time of the failure will be discarded. For our large-scale parallel training tasks, we have adopted a relatively pragmatic and hybrid technical strategy.

In general, we utilize proven cloud storage technologies to ensure reliable data storage, while also fully recognizing the separate challenges that computation and networking can present. We had an in-depth discussion with our customers and got a key message, i.e, the underlying system should not introduce any uncertainty into the model training process (*Takeaways-2*). Therefore, we have only two options for fault-tolerant computing: either perform online redundant computations or prepare backup resources to replace failed nodes. Given the high cost of GPUs, it’s more cost-effective to use backup resources rather than online redundancy for fault tolerance. Consequently, we’ve allocated 64 backup GPUs across 8 servers for every 1024 GPUs on 128 servers, ensuring identical communication and performance for parallel training on any 128 servers from this 136-server pool.

Regarding networking, the industry typically adopts single-port cards such as 1*400G to diminish the chances of hash collisions. Nonetheless, this configuration introduces reliability concerns, as a port malfunction can force tasks to restart from the most recent checkpoint. Our methodology, which reflects the insights gained from customer feedback, emphasizes swift failure detection and the maintenance of network connectivity. This strategy enables higher-layer applications to react more adeptly, such as scheduling timely restarts or initiating on-demand checkpoints that are strategically based on recent checkpointing activities. Pursuing this direction, we have opted for 2*200G dual uplinks to enhance reliability, while simultaneously addressing network hash collisions to sustain application performance. In essence, we believe that ensuring maximum reliability at each layer, coupled with cross-layer optimization, is vital for achieving the most efficient and reliable overall system (*Takeaways-3*).

Our approach: C4D. In summary, our system’s fault-tolerant architecture includes reliable data storage through erasure coding, network reliability via dual uplinks and multi-path communication, and handling of computational faults through checkpoints and redundancy. The core of this system is the C4D (C4 Diagnose) subsystem, designed to quickly detect hardware failures for prompt task restarts, as shown in Fig. 3.

C4D leverages two key observations (*Takeaways-4*): (1) parallel training tasks exhibit a regular and predictable running rhythm, enabling us to precisely identify abnormal behaviors; (2) the Bulk Synchronous Parallel (BSP) execution model in parallel training requires regular synchronization points. And these synchronization points are used as anchors for measuring anomalies.

Based on above observations, we developed the C4D to facilitate online fault detection. Fig. 4 illustrates the key elements of the C4D, which includes an enhanced Collective Communication Library (CCL), a central C4D master, and the C4a (C4 agent) that acts as an intermediary. We opt to use enhanced CCL because state-of-the-art CCLs, such

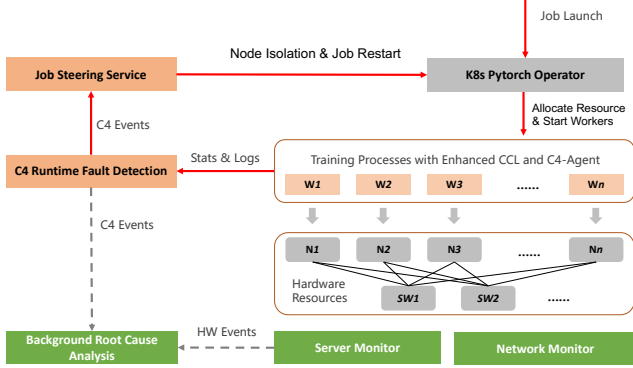


Figure 3. The overview of the fault-tolerant system.

as NCCL [20], lack the capability for online monitoring of collective communication operations.

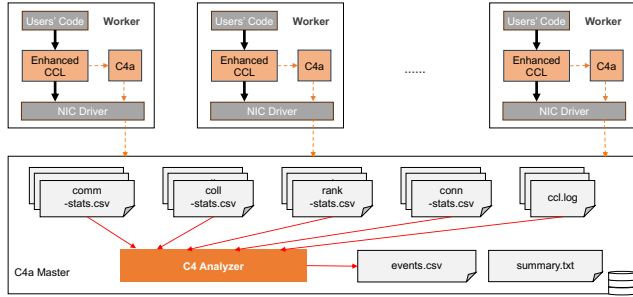


Figure 4. The architecture of C4D.

C4D Monitoring. Fig. 5 shows our enhanced CCL with four layers, similar to contemporary CCLs. We’ve expanded the bottom three layers for monitoring functionalities. The communicator layer tracks communicator IDs, rank counts, and rank assignments. The operation layer monitors collective operation types, algorithms, data types, element counts, and operation durations and counts. The transport layer gathers connection specifics like RDMA IP and QP numbers, and message statistics including counts, sizes, and durations of transfers. It’s not trivial to collect above information at runtime, with low cost and high accuracy. To precisely monitor communication kernel execution patterns, we refined all related CDUA kernels to log their start and completion times directly, as CPU timestamps and CUDA Events are ineffective or inaccurate for this purpose.

C4D analysis. Based on above gathered informations, we can detect four common types of errors that frequently occur in our clusters, i.e., *communication hang*, *non-communication hang*, *communication slow*, and *non-communication slow*. Detecting the first two error types is relatively easy and will not be discussed in-depth here, and we will focus on the more complex task of identifying instances of the *slow* syndrome.

Case 1: Communication Slow Detection. Before delving into the details, we will give a brief introduction to the

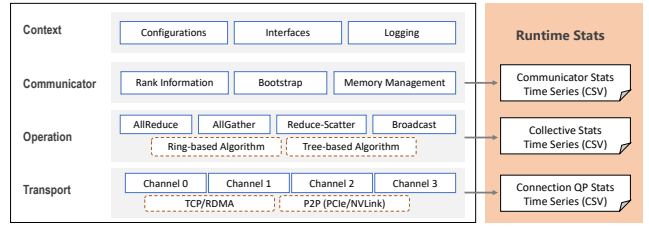


Figure 5. The Enhanced CCL.

data flow in collective communication. Considering the *allreduce* operation in data parallel phase as an example, where workers need to average gradients across all model replicas. Frameworks and CCLs will split messages into chunks and submitting them to the network sequentially. Since all workers adhere to the same data splitting rules, ensuring that message sizes remain consistent when posted to the network. Therefore, we can identify communication slowdowns at the transport layer by monitoring and comparing the latency of messages in different workers.

An illustrative example is shown in Fig. 6. Communication delays across workers are mapped into a two-dimensional matrix, where each element represents the delay between a pair of workers, identified by their y-coordinate (source) and x-coordinate (destination). High values in the matrix help identify slow connections: a single high-value point indicates a specific connection bottleneck, a row of high values suggests a problem with the source, and a column of high values points to an issue with the destination.

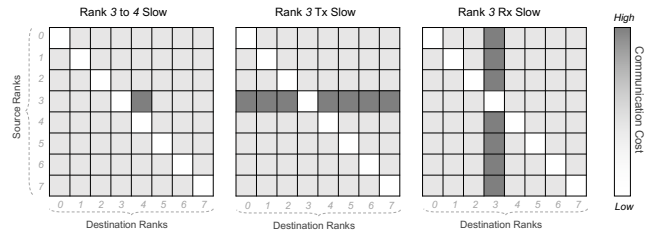


Figure 6. The symptom for communication slow.

Case 2: Non-Communication Slow Detection. Consider the *ring-based* algorithm in *allreduce* operation as an example. In this configuration, all participating workers are connected sequentially, forming a ring-like structure. Each worker only communicate with its immediate neighbors in the sequence, specifically the “previous rank” and the “next rank”. Particularly, workers receive a data chunk from the “previous rank”, perform a reduction operation with their local data chunk, and then pass the resultant data to the “next rank”. In fact, due to the requirement that the receiver must first prepare the receive buffer and notify the sender before data transmission can occur, there is an implicit “receiver-driven” scheduling logic. Therefore, we can

diagnose non-communication slows, such as those caused by computation or data loading, by looking at how long the receiver waits for data. For instance, if the receiver experiences a non-communication slow, the sender is likely already waiting, allowing for quick data receipt once scheduled. Conversely, if the sender has a non-communication slow, it won't send data promptly even after receiving the receiver's scheduling signal, resulting in lengthy wait times for the receiver.

3.2 The Scalability of Parallel Training

Parallel training performance depends on the efficiency of single-node computation, data access, and collective communication. While single-node efficiency can be improved through optimizations like mixed precision [35] and transformer engine [33], and data access efficiency through caching mechanisms like Alluxio [25], this paper focuses on collective communication efficiency, a key factor in training scalability.

If we consider network bandwidth as a resource, optimizing collective communication performance is equivalent to finding an optimal method for resource allocation. In fact, collective communication can be seen as a collection of one-to-one communications between two of the workers, which may also involve computation if a reduce operation is included. Therefore, the problem of finding an optimal resource allocation can be broken down into two issues. First, we need to minimize the resource requirements of each one-to-one communication. Second, we need to map each one-to-one communication to network resources in a way that minimizes the total communication time.

The first issue is not the focus of this paper, so for the sake of completeness, we provide a brief introduction here. Once the data volume for one-to-one communication is fixed, its consumption of network resources is directly proportional to the distance the data travels through the network. To reduce the data transmission distance, we employ two optimization strategies. First, we minimize the network diameter through innovative network architecture. AI training servers internally provide high-speed NVLINK interconnects, which are inherently part of the network (*Takeaways-5*). Thus, our network is actually a hierarchical topology, with NVLINK forming the first layer and the RDMA network across different servers comprising the second layer. Furthermore, we have utilized dual-uplink technology, which not only improves network reliability but also allows for an increase in the radix of switch chips. Clearly, for a given number of endpoints and a specified network topology, the greater the switch radix, the smaller the network diameter [22]. Second, we utilize network topology-aware scheduling techniques to ensure that the two ranks needing to communicate are as close as possible within the network.

Based on the above optimizations, we can achieve good performance in most cases. For instance, for single tasks with

a small scale, all communications can be completed within a single layer of leaf switches. But for training tasks of a larger scale or in scenarios where multiple tasks coexist, further optimization is essential. The underlying problem in both of the aforementioned scenarios is actually the same: there is a significant amount of traffic that requires forwarding by the spine switches, resulting in a high volume of traffic collisions.

Our approach: C4P. To address this challenge, we introduced the C4P (C4 Performance) system, engineered to reduce unnecessary communication costs. C4P optimizes communication for concurrent jobs and link failures by: (1) identifying and avoiding faulty links at task start-up, (2) balancing RDMA QPs, i.e., connections, across paths for load distribution, and (3) dynamically adapting QP workloads in response to network changes and traffic conflicts. Essentially, C4P is a traffic engineering technique that aims to minimize network congestion by regulating the transmission paths of each data flow within the network. This concept isn't new, but it's not commonly employed in traditional data centers, because of the massive connections in network. C4P is practical in parallel training scenarios mainly because the traffic characteristics generated by parallel training are significantly different from those of conventional cloud applications. That is, parallel training tasks involve a small number of data flows but transmit large volumes of data. This presence of a few elephant flows makes it feasible for C4P to meticulously plan the route for each data flow (*Takeways-6*).

C4P follows C4D's software structure but with key differences, as shown in Fig. 7. Firstly, the C4P master acts as a control center for multiple jobs or tenants, unlike the single-job-focused C4D master. Additionally, C4P's CCL can request path allocations for communicating workers, while C4D's collects monitoring data. Lastly, C4P's master allocates communication paths, whereas C4D's master handles fault detection and diagnosis.

Similar to prior studies [13], we use path-probing for refined traffic engineering. C4P first isolates and discards malfunctioning links between leaf and spine switches, creating a healthy-link network. The C4P master performs full-mesh path probing via randomly selected servers per leaf switch, identifying and cataloging reliable paths. On connections setup, the CCL prompts path requests to the C4P master, which responses selected path by specifying the source ports of RDMA connections. The master ensures traffic from the same NIC is balanced between left and right ports by forbidding the paths from left ports to right, and vice versa. Additionally, traffic from servers under the same leaf switch is distributed over all available spine switches to prevent network congestion. The CCL constantly evaluates message completion times on various paths and prioritizes the fastest for data transfer. If the optimal QP's queue is full, the next best is chosen. This approach helps maintain low transmission delays despite path errors or traffic congestion.

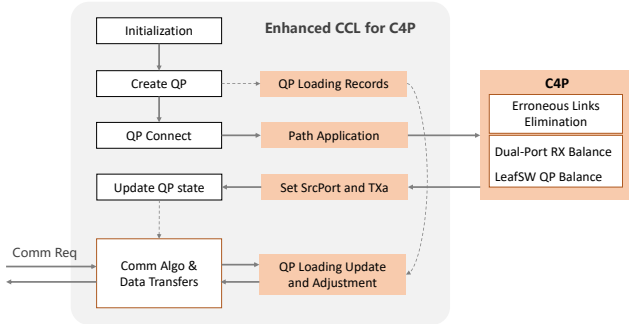


Figure 7. The working flow of C4P.

The deployment approach for C4P parallels C4D’s, with both systems embedded into user images to facilitate integration with Kubernetes (K8s). A significant distinction, however, is that the C4P master operates on a system-wide level, offering global access, in contrast to the C4D master, which serves a more localized role, restricted to individual job scopes. Details beyond this will not be reiterated here to prevent redundancy.

4 Evaluations

4.1 Setup

As shown in Table 2, we outline the system configurations of our operational clusters, from which we have gathered the evaluation data for C4D. The assessments pertaining to C4P, on the other hand, were carried out on a subset of this cluster. To prevent any interference with other ongoing jobs in the cluster and to ensure the integrity of our evaluation results, we have allocated a specific segment of the cluster as a controlled testing environment. This testbed comprises 16 nodes, equipped with a total of 128 GPUs. And all the nodes are directly connected to 8 dedicated leaf switches, ensuring an exclusive environment for our testing activities.

The nodes within this high-performance cluster are outfitted with 8 NVIDIA H800 GPUs and 8 BlueField-3 NICs [36]. Each NIC provides two physical 200Gbps ports, which are bonded to create a single logical 400Gbps port. These NICs are integrated into a 3-Tier Clos network [7], configured in a Fat-Tree topology with a 1:1 oversubscription rate, ensuring optimal performance and bandwidth distribution. Leveraging Broadcom’s Trident4 [4] as leaf and Tomahawk4 as spine switches [3], the cluster is capable of supporting over 10,000 GPUs. In a single pod, which constitutes a two-tier subnet, it can accommodate 512 GPUs, showcasing its expansive scalability.

The effectiveness of C4D is evaluated with one of our real-world LLM training workloads. And the model for this job contains 175 billion parameters. Undertaking distributed training with 2400 GPUs, the model typically requires over a month for a complete training cycle from scratch. In contrast, the efficiency of C4P is assessed using both collective

Table 2. Configurations

Benchmarks for C4D	GPT model, 175 billion parameters
	allreduce operations
Benchmarks for C4P	GPT model, 22 billion parameters
	Llama model, 13 billion parameters
	GPT model, 175 billion parameters
Frameworks	Megatron-LM [47], DeepSpeed [43]
Nodes	NV H800 * 8, BlueField3 * 8 (200Gbps * 2)
Network	3-Tier Clos, Fat-Tree, 1:1 oversubscription rate

communication benchmarks and three representative LLM training jobs. To ensure unbiased evaluation results for the communication benchmarks, we configured them to utilize a ring-based algorithm. The specific configurations of the models involved in the testing, such as parallel strategy and zero-optimizer level, will be detailed alongside the presentation of the evaluation outcomes.

4.2 Results

4.2.1 The Evaluations on C4D’s Effectiveness. We have reviewed the historical logs of the jobs from one of our inner customers, including their start and terminated timestamps, and whether a job is succeeded or failed by some reasons. Our primary emphasis has been placed on a representative job that demands 2400 GPUs and necessitates over a month to complete its model training process. As shown in Table 3, we compare the error-induced downtime of this job before (Jun, 2023) and after (Dec, 2023) the proposed fault-tolerant system was deployed. The data clearly indicates that the deployment of C4D led to a substantial decrease in downtime, with an approximately 30x reduction, from 31.19% down to just 1.16%.

The downtime in in June 2023 is broken down into four parts, according to the classification in Fig. 1. It reveals that the majority of the downtime was due to extended periods of system diagnosis. This was largely because identifying the precise cause of job failure could take hours or even days in the absence of our purpose-built diagnostic tools. The second major contributor to downtime was post-checkpoint overhead. That is because the users often scheduled infrequent checkpoints to save the model parameters, not anticipating high error rates in a large-scale training cluster. This led to a significant amount of computing activity being rendered useless between the last valid checkpoint and the moment the job failed due to an error. To address this issue and reduce the amount of wasted computing time, users have begun saving checkpoints more frequently by taking advantage of the high-performance infrastructure provided [51]. Besides the diagnosing and post-checkpoint cost, there is also 3.4% of time spent on crash detection. Typically, users are not immediately aware that their job has stalled following an error event. For instance, PyTorch jobs that might experience a hang for up to 30 minutes, until the elastic agent [40]

Table 3. Error-induced Downtime Statistics

Error-induced Downtime in Jun, 2023			
Post-Checkpoint	7.53%		
Detection	3.41%		
Diagnosis & Isolation	19.65%	ECC/NVLink Error	8.34%
		CUDA Error	4.19%
		NCCL Timeout	3%
		ACK Timeout	1.8%
Unknown	2.29%		
Re-Initialization	0.6%		
Total	31.19%		

Error-induced Downtime in Dec, 2023			
Post-Checkpoint	0.23%		
Detection	0.05%		
Diagnosis & Isolation	0.73%	ECC/NVLink Error	0.2%
		CUDA Error	0.1%
		NCCL Timeout	0.23%
		ACK Timeout	0.1%
Unknown	0.1%		
Re-Initialization	0.15%		
Total	1.16%		

kills the processes. This delay creates a span of idle time for computing resources, and thus constitutes a non-negligible portion of the total downtime.

In December 2023, despite system diagnosis continuing to account for the majority of downtime, its contribution had been reduced by approximately 27x compared to past performance, which is somewhat lower than the average efficiency gains observed. The deployment of C4D has markedly accelerated both error detection and the pinpointing of faulty components, cutting down the response time to mere tens of seconds. Nevertheless, additional minutes are still required by the steering service to isolate the affected nodes and restart the job, indicating room for further improvement. The second leading cause of downtime remains the post-checkpoint duration. However, with the adoption of more frequent checkpointing, users can now save checkpoints every 10 minutes. As a result, the post-checkpoint downtime has been significantly reduced by 33x. The cost associated with job re-initialization has remained constant. It has decreased from 0.6% to 0.15% of the total time, because the average error rate has decreased by 3.33x, after the most vulnerable components of the system were identified and enhanced during this 6 months.

Upon delving deeper into the diagnosis and isolation overhead, it has become apparent that the majority of errors are attributable to GPU defects. These include GPU ECC Errors, NVLink Errors, and CUDA Errors. In June 2023, such GPU-related issues were responsible for 12.53% of the total downtime, which constituted around 2/3 of the overall

overhead. Notably, by December 2023, the incidence of these GPU-related errors had been reduced by 3.2x, while the associated time overhead saw a more dramatic decrease by 41.8x. This significant improvement can be credited to the effectiveness of C4D in handling these specific types of errors, allowing for a substantial reduction in corresponding overheads. Regarding other types of errors that are only partially manageable by C4D, there was still a noteworthy improvement. The frequency of these errors was decreased by 3.4x, and the time spent addressing them saw a reduction by 16.5x. These numbers underscore the positive impact of C4D on overall system performance and reliability.

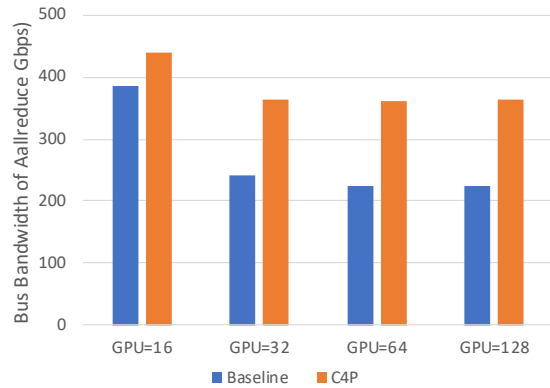


Figure 8. Improvement from balanced traffic between bonded ports.

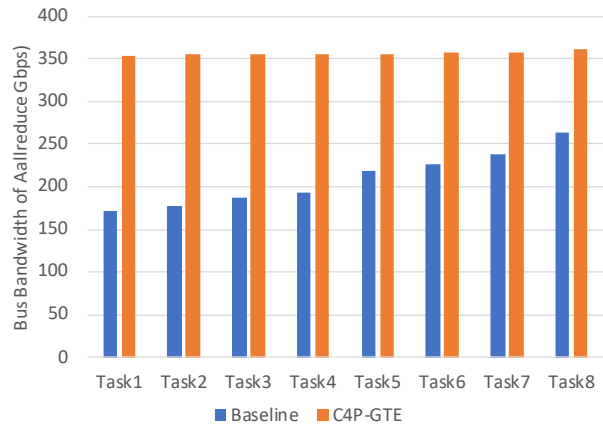
4.2.2 The Evaluations on C4P’s Effectiveness. Balancing traffic between the two bonded physical ports. As discussed in Section 3.2, when flows are dispatched from two distinct physical ports constituting a single bonded port, there is a possibility that both flows could be routed to the same physical port on the receiving end, leading to an imbalance of traffic between the two physical ports in receivers. By employing C4P, we can designate a dedicated path for the flows in each physical port, thus preventing performance degradation caused by such imbalances. Running “nccltest”, the collective operation benchmarking tool supplied by NVIDIA, we are able to measure the average *busbw*, a metric that reflects the effective communication performance (higher *busbw* means lower communication delay). Fig. 8 shows the performance of a single *allreduce* operation with and without C4P enabled. Here, the results from the two-node (16-GPU) test case don’t align with the effective bandwidth observed in the network. This discrepancy can be attributed to the methodology employed to calculate *busbw* within the benchmarks. We will not delve into this particular issue in this paper, and instead concentrate on other test cases to better illustrate our research outcomes. Without C4P, the effective *busbw* is lower than 240 Gbps in most test cases, which is far from the ideal bandwidth of

network (around 360 Gbps). However, with C4P activated, the effective *busbw* increases close to the peak value 360 Gbps, which means 50% performance gain, showcasing the tangible benefits of C4P in optimizing network performance.

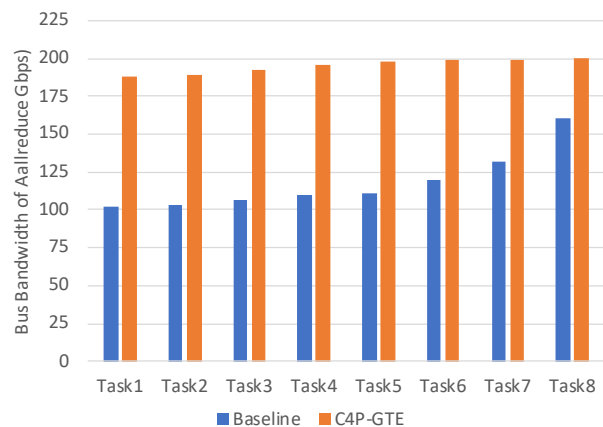
Balancing traffic among multiple jobs. To demonstrate the efficacy of C4P in alleviating traffic collisions across multiple concurrent jobs, we conducted an evaluation involving 8 simultaneous *allreduce* benchmarking applications. Each job was assigned two servers that are connected to distinct groups of leaf switches, ensuring that the traffic between workers traversed the spine switches. With 8 concurrent jobs in play, the network bandwidth was expected to be saturated by these parallel flows. Under these conditions, any suboptimal path selection could lead to an imbalanced traffic distribution, with some of the network links are overloaded. Such imbalances can severely impact the performance of collective communication, making the role of C4P crucial in maintaining peak communication performance and preventing potential bottlenecks within the network infrastructure.

Fig. 9a illustrates the performance outcomes of running concurrent *allreduce* benchmarks within a network that maintains a 1:1 oversubscription rate. The data indicates that all tasks exhibit similar levels of performance with C4P enabling global traffic engineering, closely approaching the maximum achievable throughput for a single task on this testbed. Specifically, the performance metrics for these tasks range between 353.86 Gbps and 360.57 Gbps. In contrast, when C4P is not enabled, there is a substantial performance degradation and variation among the tasks. The lowest-performing task achieves only 171.93 Gbps, while the best-performing task reaches 263.27 Gbps. On average, C4P improves the overall system throughput by 70.3%. This comparison clearly highlights the substantial improvements in bandwidth utilization and consistency enabled by C4P.

It is important to clarify that the peak throughput in this system is constrained by the NVLink fabric, causing the maximum attainable bus bandwidth at 362 Gbps. Because of the limitation of NVLink fabric, the network’s capacity is underutilized, which results in an absence of queue buildup in switches and congestion-induced transmission rate reduction in senders. To evaluate the performance of C4P within a congested network environment, we intentionally reduced the number of active spine switches by half, effectively increasing the network oversubscription rate to 2:1. Under this new configuration, we replicated the previous experiments to observe how C4P handles increased traffic conditions. The outcomes of these tests are presented in Fig. 9b. A similar conclusion can be drawn from these outcomes, with the notable exception that the performance of concurrent tasks exhibits slight variations, even when C4P is enabled. Specifically, we observe a small gap of just 11.27 Gbps between the highest and lowest throughputs. This difference is attributed to the congestion control mechanism in RDMA NICs, which dynamically adjusts the data transmission rate at the



(a) Allreduce Performance in the network with 1:1 oversubscription.



(b) Allreduce Performance in the network with 2:1 oversubscription.

Figure 9. Effectiveness of global traffic engineering.

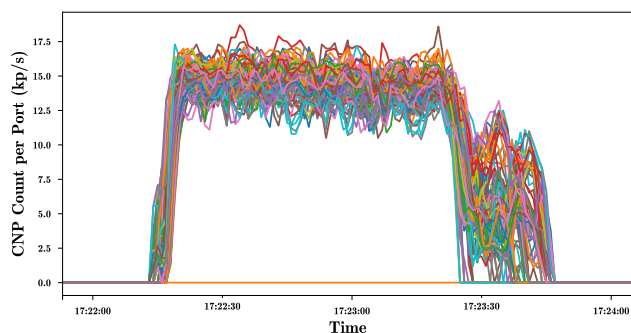
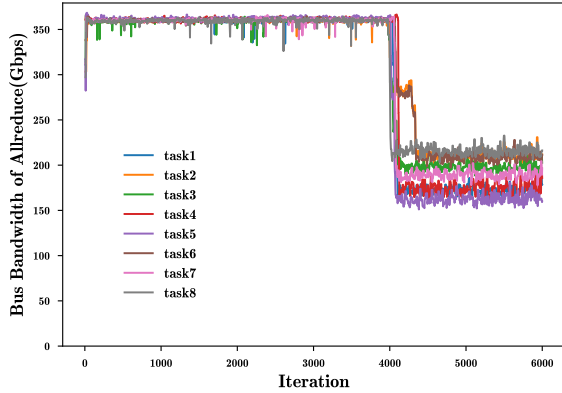
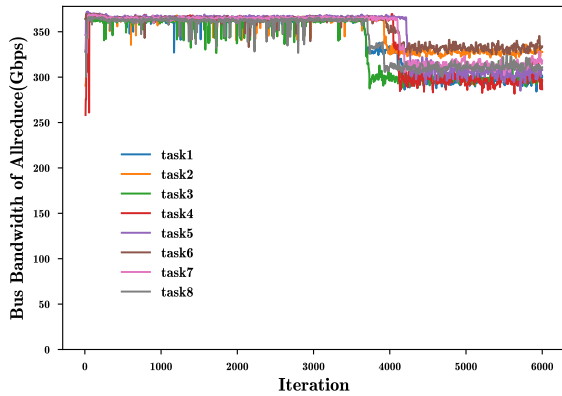


Figure 10. The CNP count received in each bonded port.

sender side in response to network conditions. As depicted in Fig. 10, each bonded port receives approximately 15,000 Congestion Notification Packets (CNPs) every second, with the count fluctuating between 12,500 and 17,500. The arrival of CNPs instigates a throttling of the data transfer rate from the



(a) Allreduce Performance with C4P static traffic engineer.

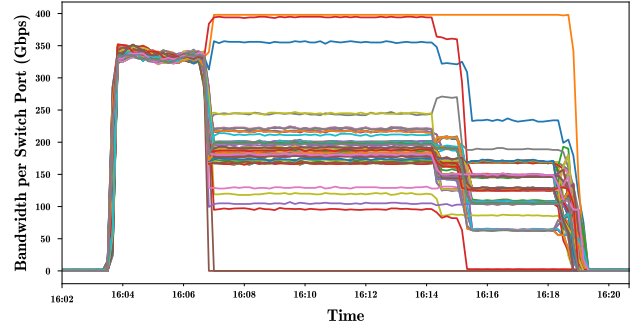


(b) Allreduce Performance with C4P dynamic load balance.

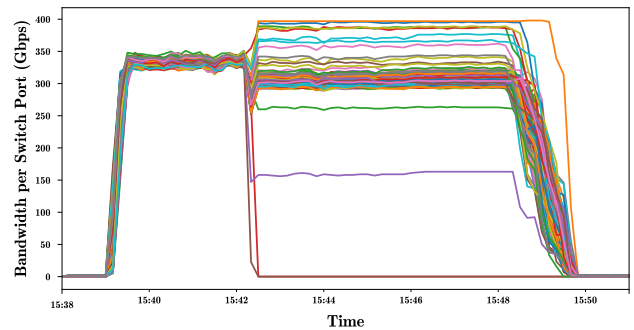
Figure 11. Effectiveness of load balance when link failure appears.

senders. Fluctuations in the frequency at which these CNPs are received directly contribute to the observed variability in the flows’ effective bandwidth. Despite these variations, the overall throughput is substantially improved by 65.55%, and the long-tail problem is obviously alleviated, with C4P enabled.

Tolerance to dynamic link failures. The efficacy of global traffic engineering relies on the stability of the underlying network conditions. A downed link can necessitate the rerouting of impacted flows, which could lead to imbalanced traffic distribution within the network, and dismiss the efficacy of global traffic engineering. In this case, load balance mechanism would take into effect to adjust the load on each flow, thereby rebalancing network traffic. To assess the effectiveness of this mechanism, we replicated previous experiments in a 1:1 oversubscribed network and intentionally deactivated a link during the experiments. To obtain the tasks’ instant performance, other than averaged value after the tasks are finished, we refined our testing benchmark to output results immediately upon completion of each



(a) Bandwidth per switch port with C4P static traffic engineer.



(b) Bandwidth per switch port with C4P dynamic load balance.

Figure 12. Comparison on switch port bandwidth with/without load balance.

allreduce operation. And the evaluation results are shown in Fig. 11. Though high-frequency timestamp recording results in some fluctuations in the data, we can still observe significant improvement in system throughput, with dynamic load balance enabled. In the tests that C4P load balancing is not activated, the bus bandwidth for the given tasks experiences considerable degradation, with values ranging between 160 Gbps and 220 Gbps and an average bandwidth of 185.76 Gbps. Conversely, when C4P load balancing is enabled, the observed bus bandwidth improves significantly, ranging from 290 Gbps to 335 Gbps, with an average of 301.46 Gbps. This enhancement represents a substantial performance gain of 62.3% when a link error occurs during the training processes. Note that, with 1 link error among the 8 uplinks, the theoretical ideal performance would be 7/8 of the original, i.e., 315 Gbps. And the performance achieved with C4P enabled is found to be in close proximity to this ideal value.

To demonstrate how C4P load balance improves the system throughput, we have collected the statistics from the leaf switches regarding the traffic distribution across each port, as illustrated in Fig. 12. With C4P traffic engineering implemented, all upstream ports exhibit near-optimal bandwidth utilization prior to the induction of a link error. However,

the emergence of the link error leads to a marked discrepancy in throughput across different ports. In the absence of C4P load balancing, only three of the ports exhibit traffic increment, indicating that the flows intended for the disabled link are being rerouted to these ports. As a result, the available bandwidth for each flow in these congested ports is reduced, and the performance of the flows in the same communication channel is also negatively affected. Consequently, a noticeable reduction in bandwidth is observed in the other ports. Conversely, C4P load balancing dynamically adjusts the distribution of network traffic, decreasing the burden on congested flows while increasing it on those traversing underutilized paths. This strategy leads to a more balanced load across the ports, which allows those that were previously underutilized to handle more traffic. Thus, this optimization results in an overall enhancement of the system’s throughput.

Performance improvement in real-life jobs. To evaluate the efficacy of C4P in enhancing the performance of real-world applications, we conducted tests using three representative training jobs: Job1 involves training a GPT model utilizing the Megatron framework, incorporating both TP and DP strategies for distributed training. This model comprises 22 billion parameters, and the TP and DP sizes are set to 8 and 16, respectively. Job2 trains a Llama model, which contains 7 billion parameters. For this task, the Deepspeed framework is employed for distributed training. The zero-optimization [43] is activated, with the training leveraging only DP. Job3 entails training another GPT model with 175 billion parameters. This model is also trained based on Megatron framework, using both TP and PP strategies. With both TP and PP sizes configured as 8, it effectively creates 2 DP groups.

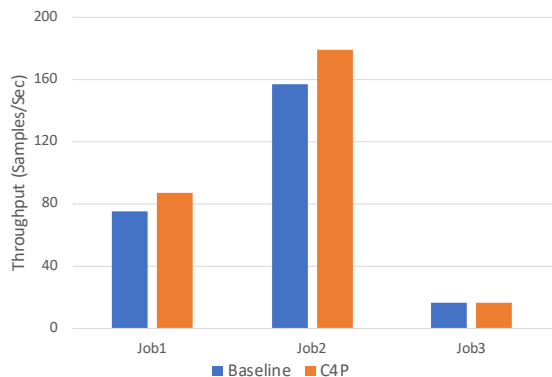


Figure 13. Performance improvement in real-life jobs.

The performance evaluation results are depicted in Fig. 13. As can be discerned from the figure, significant improvements in the performance of the first two jobs. Specifically, the throughput of Job1 has increased by 15.95%, rising from 74.82 to 86.76 samples per second. Similarly, Job2 shows

an enhancement of 14.1%, with throughput climbing from 156.59 to 178.65 samples per second. In contrast, Job3 does not exhibit a noticeable improvement in performance. Our analysis suggests that the discrepancy in performance gains is closely associated with the proportion of communication time within a training step. For the first two jobs, the communication overhead constitutes over 30% of each iteration’s duration. However, Job3 is configured with a high Gradient Accumulation (GA) value of 16, which implies that parameter updates occur only once every 16 steps. This setting substantially reduces the relative communication cost, which explains the minimal performance improvement observed for Job3.

5 Related Works

To better utilize GPU resources in LLM training, existing research makes effort in two dimensions: stability improvement and performance improvement.

Improving stability by monitoring and fault tolerance. Existing research on data center monitoring primarily focuses on general applications within data centers [21, 24, 55], focusing on the behavior of hardware components such as CPUs, RDMA NICs, and switches. However, when compared to conventional data center applications, the training of LLMs is characteristically on a much larger scale and involves more complex interactions between software and hardware modules. This complexity necessitates more sophisticated, high-granularity monitoring solutions [38, 44] that are integrated within the software stack.

In terms of fault tolerance, the prevalent approach is the use of in-memory checkpointing [15, 29, 31, 52]. These efforts copy the current LLM states to the host memory with high frequency such as one checkpoint per iteration. In the event of an error, once the issue has been identified, training can resume from the most recent checkpoint.

Improving performance by better training architectures and network. With given computation resources, the performance of LLM training can be improved by multiple-layer efforts, including (from the higher layer to the lower layer) training architectures, communication libraries, and network structure. The LLM training tries to parallelize GPU computation with communication and CPU operations [44, 46, 56], or change the behavior of LLM training to reduce the overload, leveraging the properties of specific model structures [9, 26]. Communication libraries try to better utilize the given network bandwidth, including NVLink, PCIe, and RNIC, to shorten the delay of a data transmission [13, 16, 20, 28], or design better strategies to aggregate data in collective communication [6, 8, 45]. Network structure research explore reasonable topologies to connect multiple hosts with appropriate bandwidth, providing better performance in LLM training.

6 discussion

Adaptive routing [10] and packet spraying [12] generally point to the same solution, which involves performing per-packet load balancing within switches based on network conditions. This approach holds advantages over traditional ECMP technology as it can effectively address imbalances in network bandwidth utilization caused by large flow hash collisions. However, implementing such techniques introduces complexities for RoCE networks and higher-level applications. For instance, to alleviate the pressure on RNIC's on-chip buffers due to out-of-order packets, NVIDIA's RNIC only enable adaptive routing for RDMA Write operations [37]. Consequently, all RDMA Write packets are transformed into RDMA Write Only packets, ensuring each packet carries the destination DMA address. Furthermore, to preserve the ordering required by upper-layer applications for RDMA operations, the final packet must use the RDMA Write with immediate operation, and it can only be sent after all preceding packets have been acknowledged. This safeguards the integrity of the Completion Queue Entry (CQE) generation, ensuring that all data from Write operations is properly committed to memory. These constraints necessitate careful adaptation of upper-layer software to enable adaptive routing. Currently, AR support has been integrated into NCCL, and has been successfully verified on InfiniBand networks. Despite our active exploration of this technology, it has not achieved widespread adoption, primarily due to two significant reasons. First, AR on RoCE depends on underlying hardware and requires the latest switches and RNICs for support. Second, AR technology relies on a lossless RDMA network, which can exacerbate congestion when endpoint congestion occurs, potentially paralyzing the entire cluster network [17]. Actually, to avoid the operational risks associated with lossless networks, we have extensively deployed lossy RDMA networks. Achieving optimal AR performance in lossy RDMA networks is also a problem we are currently exploring.

7 Conclusion

Achieving optimal performance in training LLMs within large-scale AI clusters is challenging, hindered by frequent errors and traffic congestion. To address these issues, we have developed C4, a communication-centric solution designed to minimize system downtime and enhance communication efficiency. By leveraging the characteristics of distributed training, C4 can substantially reduce the system recovery cost when faced with non-correctable errors. It achieves this through rapid online fault detection, immediate isolation of anomalies, and by working in synergy with regular checkpoints and automated restart mechanisms. Additionally, C4 employs the predictable patterns of collective communication to implement precise traffic management, which greatly alleviates network congestion. C4 can reduce error-induced

overhead by roughly 30% and improve their throughput by about 15% for tested applications with moderate communication costs.

References

- [1] Marcos Kawazoe Aguilera, Ramaprabhu Janakiraman, and Lihao Xu. 2005. Using erasure codes efficiently for storage in a distributed system. In *2005 International Conference on Dependable Systems and Networks (DSN'05)*. IEEE, 336–345.
- [2] Jinze Bai, Shuai Bai, Yunfei Chu, Zeyu Cui, Kai Dang, Xiaodong Deng, Yang Fan, Wenbin Ge, Yu Han, Fei Huang, Binyuan Hui, Luo Ji, Mei Li, Junyang Lin, Runji Lin, Dayiheng Liu, Gao Liu, Chengqiang Lu, Keming Lu, Jianxin Ma, Rui Men, Xingzhang Ren, Xuancheng Ren, Chuanqi Tan, Sinan Tan, Jianhong Tu, Peng Wang, Shijie Wang, Wei Wang, Shengguang Wu, Benfeng Xu, Jin Xu, An Yang, Hao Yang, Jian Yang, Shusheng Yang, Yang Yao, Bowen Yu, Hongyi Yuan, Zheng Yuan, Jianwei Zhang, Xingxuan Zhang, Yichang Zhang, Zhenru Zhang, Chang Zhou, Jingren Zhou, Xiaohuan Zhou, and Tianhang Zhu. 2023. Qwen Technical Report. (2023). arXiv:cs.CL/2309.16609
- [3] BROADCOM. [n. d.]. Tomahawk4 / BCM56990 Series. ([n. d.]). <https://www.broadcom.com/products/ethernet-connectivity/switching/strataxgs/bcm56990-series>.
- [4] BROADCOM. [n. d.]. Trident4 / BCM56880 Series. ([n. d.]). <https://www.broadcom.com/products/ethernet-connectivity/switching/strataxgs/bcm56880-series>.
- [5] Tom Brown, Benjamin Mann, Nick Ryder, Melanie Subbiah, Jared D Kaplan, Prafulla Dhariwal, Arvind Neelakantan, Pranav Shyam, Girish Sastry, Amanda Askell, et al. 2020. Language models are few-shot learners. *Advances in neural information processing systems* 33 (2020), 1877–1901.
- [6] Zixian Cai, Zhengyang Liu, Saeed Maleki, Madanlal Musuvathi, Todd Mytkowicz, Jacob Nelson, and Olli Saarikivi. 2021. Synthesizing optimal collective algorithms. In *Proceedings of the 26th ACM SIGPLAN Symposium on Principles and Practice of Parallel Programming*. 62–75.
- [7] Charles Clos. 1953. A study of non-blocking switching networks. *The Bell System Technical Journal* 32, 2 (1953), 406–424. <https://doi.org/10.1002/j.1538-7305.1953.tb01433.x>
- [8] Meghan Cowan, Saeed Maleki, Madanlal Musuvathi, Olli Saarikivi, and Yifan Xiong. 2023. MSCCLang: Microsoft Collective Communication Language. In *Proceedings of the 28th ACM International Conference on Architectural Support for Programming Languages and Operating Systems, Volume 2*. 502–514.
- [9] Weihao Cui, Zhenhua Han, Lingji Ouyang, Yichuan Wang, Ningxin Zheng, Lingxiao Ma, Yuqing Yang, Fan Yang, Jilong Xue, Lili Qiu, et al. 2023. Optimizing dynamic neural networks with brainstorm. In *17th USENIX Symposium on Operating Systems Design and Implementation (OSDI 23)*. 797–815.
- [10] Dally and Seitz. 1987. Deadlock-Free Message Routing in Multiprocessor Interconnection Networks. *IEEE Trans. Comput.* C-36, 5 (1987), 547–553. <https://doi.org/10.1109/TC.1987.1676939>
- [11] Alexandros G Dimakis, Vinod Prabhakaran, and Kannan Ramchandran. 2006. Decentralized erasure codes for distributed networked storage. *IEEE Transactions on Information Theory* 52, 6 (2006), 2809–2816.
- [12] Advait Dixit, Pawan Prakash, Y. Charlie Hu, and Ramana Rao Kompella. 2013. On the impact of packet spraying in data center networks. In *2013 Proceedings IEEE INFOCOM*. 2130–2138. <https://doi.org/10.1109/INFCOM.2013.6567015>
- [13] Jianbo Dong, Shaochuang Wang, Fei Feng, Zheng Cao, Heng Pan, Lingbo Tang, Pengcheng Li, Hao Li, Qianyuan Ran, Yiqun Guo, et al. 2021. ACCL: architecting highly scalable distributed training systems with highly efficient collective communication library. *IEEE Micro* (2021).

- [14] Zhengxiao Du, Yujie Qian, Xiao Liu, Ming Ding, Jiezhong Qiu, Zhilin Yang, and Jie Tang. 2022. GLM: General Language Model Pretraining with Autoregressive Blank Infilling. (2022). arXiv:2103.10360
- [15] Assaf Eisenman, Kiran Kumar Matam, Steven Ingram, Dheevatsa Mudigere, Raghuraman Krishnamoorthi, Krishnakumar Nair, Misha Smelyanskiy, and Murali Annavam. 2022. {Check-N-Run}: A checkpointing system for training deep learning recommendation models. In *19th USENIX Symposium on Networked Systems Design and Implementation (NSDI 22)*. 929–943.
- [16] Facebook. 2023. Gloo. (2023). <https://github.com/facebookincubator/gloo>.
- [17] Binzhang Fu and John Kim. 2017. Footprint: Regulating routing adaptiveness in Networks-on-Chip. In *2017 ACM/IEEE 44th Annual International Symposium on Computer Architecture (ISCA)*. 691–702. <https://doi.org/10.1145/3079856.3080249>
- [18] Huaizhong Han, Srinivas Shakkottai, C. V. Hollot, R. Srikant, and Don Towsley. 2006. Multi-Path TCP: A Joint Congestion Control and Routing Scheme to Exploit Path Diversity in the Internet. *IEEE/ACM Transactions on Networking* 14, 6 (2006), 1260–1271. <https://doi.org/10.1109/TNET.2006.886738>
- [19] C. Hopps. 2000. RFC2992: Analysis of an Equal-Cost Multi-Path Algorithm. (2000).
- [20] Sylvain Jeaugey. 2017. Nccl 2.0. In *GPU Technology Conference (GTC)*, Vol. 2.
- [21] Raj Joshi, Ting Qu, Mun Choon Chan, Ben Leong, and Boon Thau Loo. 2018. BurstRadar: Practical real-time microburst monitoring for datacenter networks. In *Proceedings of the 9th Asia-Pacific Workshop on Systems*. 1–8.
- [22] John Kim. 2008. *High-radix interconnection networks*. Ph.D. Dissertation. Stanford, CA, USA. Advisor(s) Dally, William J. AAI3302840.
- [23] Richard Koo and Sam Toueg. 1987. Checkpointing and rollback-recovery for distributed systems. *IEEE Transactions on software Engineering* 1 (1987), 23–31.
- [24] Mahendra Kutare, Greg Eisenhauer, Chengwei Wang, Karsten Schwan, Vanish Talwar, and Matthew Wolf. 2010. Monalytics: online monitoring and analytics for managing large scale data centers. In *Proceedings of the 7th international conference on Autonomic computing*. 141–150.
- [25] Haoyuan Li. 2018. *Alluxio: A Virtual Distributed File System*. Ph.D. Dissertation. EECS Department, University of California, Berkeley. <http://www2.eecs.berkeley.edu/Pubs/TechRpts/2018/EECS-2018-29.html>
- [26] Juncai Liu, Jessie Hui Wang, and Yimin Jiang. 2023. Janus: A Unified Distributed Training Framework for Sparse Mixture-of-Experts Models. In *Proceedings of the ACM SIGCOMM 2023 Conference*. 486–498.
- [27] Yuanwei Lu, Guo Chen, Bojie Li, Kun Tan, Yongqiang Xiong, Peng Cheng, Jiansong Zhang, Enhong Chen, and Thomas Moscibroda. 2018. Multi-Path Transport for RDMA in Datacenters. In *15th USENIX Symposium on Networked Systems Design and Implementation (NSDI 18)*. USENIX Association, Renton, WA, 357–371. <https://www.usenix.org/conference/nsdi18/presentation/lu>
- [28] Microsoft. 2023. NSCCL. (2023). <https://github.com/microsoft/msccl>.
- [29] Jayashree Mohan, Amar Phanishayee, and Vijay Chidambaram. 2021. {CheckFreq}: Frequent, {Fine-Grained} {DNN} Checkpointing. In *19th USENIX Conference on File and Storage Technologies (FAST 21)*. 203–216.
- [30] Shubhendu S Mukherjee, Michael Kontz, and Steven K Reinhardt. 2002. Detailed design and evaluation of redundant multithreading alternatives. *ACM SIGARCH Computer Architecture News* 30, 2 (2002), 99–110.
- [31] Bogdan Nicolae, Jiali Li, Justin M Wozniak, George Bosilca, Matthieu Dorier, and Franck Cappello. 2020. Deepfreeze: Towards scalable asynchronous checkpointing of deep learning models. In *2020 20th IEEE/ACM International Symposium on Cluster, Cloud and Internet Computing (CCGRID)*. IEEE, 172–181.
- [32] NVIDIA. [n. d.]. NVIDIA A100 Tensor Core GPU. ([n. d.]). <https://www.nvidia.com/en-us/data-center/a100/>.
- [33] NVIDIA. [n. d.]. NVIDIA BLUEFIELD-3 DPU. ([n. d.]). <https://www.nvidia.com/content/dam/en-zz/Solutions/Data-Center/documents/datasheet-nvidia-bluefield-3-dpu.pdf>.
- [34] NVIDIA. [n. d.]. NVIDIA H100 Tensor Core GPU. ([n. d.]). <https://www.nvidia.com/en-us/data-center/h100/>.
- [35] NVIDIA. [n. d.]. Train With Mixed Precision. ([n. d.]). <https://docs.nvidia.com/deeplearning/performance/mixed-precision-training/index.html>.
- [36] NVIDIA. [n. d.]. Transformer Engine documentation. ([n. d.]). <https://docs.nvidia.com/deeplearning/transformer-engine/user-guide/index.html>.
- [37] Nvidia. 2023. HOW TO CONFIGURE ADAPTIVE ROUTING AND SELF-HEALING NETWORKING (NEW). (2023). <https://enterprise-support.nvidia.com/s/article/How-To-Configure-Adaptive-Routing-and-Self-Healing-Networking-New>.
- [38] Nvidia. 2023. Nvidia Nsight Systems. (2023). <https://developer.nvidia.com/nsight-systems>.
- [39] Stefan Poledna. 2007. *Fault-tolerant real-time systems: The problem of replica determinism*. Vol. 345. Springer Science & Business Media.
- [40] Pytorch. [n. d.]. ELASTIC AGENT. ([n. d.]). <https://pytorch.org/docs/stable/elastic/agent.html>.
- [41] Alec Radford, Karthik Narasimhan, Tim Salimans, Ilya Sutskever, et al. 2018. Improving language understanding by generative pre-training. (2018).
- [42] Alec Radford, Jeffrey Wu, Rewon Child, David Luan, Dario Amodei, Ilya Sutskever, et al. 2019. Language models are unsupervised multi-task learners. *OpenAI blog* 1, 8 (2019), 9.
- [43] Samyam Rajbhandari, Jeff Rasley, Olatunji Ruwase, and Yuxiong He. 2020. ZeRO: Memory Optimizations Toward Training Trillion Parameter Models. (2020). arXiv:cs.LG/1910.02054
- [44] Jeff Rasley, Samyam Rajbhandari, Olatunji Ruwase, and Yuxiong He. 2020. Deepspeed: System optimizations enable training deep learning models with over 100 billion parameters. In *Proceedings of the 26th ACM SIGKDD International Conference on Knowledge Discovery & Data Mining*. 3505–3506.
- [45] Aashaka Shah, Vijay Chidambaram, Meghan Cowan, Saeed Maleki, Madan Musuvathi, Todd Mytkowicz, Jacob Nelson, Olli Saarikivi, and Rachee Singh. 2023. {TACCL}: Guiding Collective Algorithm Synthesis using Communication Sketches. In *20th USENIX Symposium on Networked Systems Design and Implementation (NSDI 23)*. 593–612.
- [46] Mohammad Shoeybi, Mostofa Patwary, Raul Puri, Patrick LeGresley, Jared Casper, and Bryan Catanzaro. 2019. Megatron-Lm: Training multi-billion parameter language models using model parallelism. *arXiv preprint arXiv:1909.08053* (2019).
- [47] Mohammad Shoeybi, Mostofa Patwary, Raul Puri, Patrick LeGresley, Jared Casper, and Bryan Catanzaro. 2020. Megatron-LM: Training Multi-Billion Parameter Language Models Using Model Parallelism. (2020). arXiv:cs.CL/1909.08053
- [48] Jared C. Smolens, Brian T. Gold, Babak Falsafi, and James C. Hoe. 2006. Reunion: Complexity-Effective Multicore Redundancy. In *2006 39th Annual IEEE/ACM International Symposium on Microarchitecture (MICRO'06)*. 223–234. <https://doi.org/10.1109/MICRO.2006.42>
- [49] Hugo Touvron, Thibaut Lavril, Gautier Izacard, Xavier Martinet, Marie-Anne Lachaux, Timothée Lacroix, Baptiste Rozière, Naman Goyal, Eric Hambro, Faisal Azhar, Aurelien Rodriguez, Armand Joulin, Edouard Grave, and Guillaume Lample. 2023. LLaMA: Open and Efficient Foundation Language Models. (2023).
- [50] Leslie G. Valiant. 1990. A bridging model for parallel computation. *Commun. ACM* 33, 8 (aug 1990), 103–111. <https://doi.org/10.1145/79173.79181>
- [51] Zhuang Wang, Zhen Jia, Shuai Zheng, Zhen Zhang, Xinwei Fu, TS Eugene Ng, and Yida Wang. 2023. Gemini: Fast failure recovery in

- distributed training with in-memory checkpoints. In *Proceedings of the 29th Symposium on Operating Systems Principles*. 364–381.
- [52] Zhuang Wang, Zhen Jia, Shuai Zheng, Zhen Zhang, Xinwei Fu, TS Eugene Ng, and Yida Wang. 2023. Gemini: Fast failure recovery in distributed training with in-memory checkpoints. In *Proceedings of the 29th Symposium on Operating Systems Principles*. 364–381.
- [53] Hakim Weatherspoon and John D Kubiatowicz. 2002. Erasure coding vs. replication: A quantitative comparison. In *International Workshop on Peer-to-Peer Systems*. Springer, 328–337.
- [54] Mingyuan Xia, Mohit Saxena, Mario Blaum, and David A. Pease. 2015. A Tale of Two Erasure Codes in HDFS. In *13th USENIX Conference on File and Storage Technologies (FAST 15)*. USENIX Association, Santa Clara, CA, 213–226. <https://www.usenix.org/conference/fast15/technical-sessions/presentation/xia>
- [55] Curtis Yu, Cristian Lumezanu, Abhishek Sharma, Qiang Xu, Guofei Jiang, and Harsha V Madhyastha. 2015. Software-defined latency monitoring in data center networks. In *Passive and Active Measurement: 16th International Conference, PAM 2015, New York, NY, USA, March 19-20, 2015, Proceedings 16*. Springer, 360–372.
- [56] Chen Zhang, Lingxiao Ma, Jilong Xue, Yining Shi, Ziming Miao, Fan Yang, Jidong Zhai, Zhi Yang, and Mao Yang. 2023. Cocktail: Analyzing and Optimizing Dynamic Control Flow in Deep Learning. In *17th USENIX Symposium on Operating Systems Design and Implementation (OSDI 23)*. 681–699.